

Original Article

A multidimensional analysis of ZW10 interacting kinetochore protein in human tumors

Yufeng Shu^{1*}, Xiaoyang Pang^{2*}, Huan Li¹, Chao Deng³

¹Department of Gastroenterology, Third Xiangya Hospital, Central South University, Changsha, Hunan, China;

²Department of Spinal Surgery, Xiangya Hospital, Central South University, Changsha, Hunan, China; ³Department of Orthopedics, Xiangya Hospital, Central South University, Changsha, Hunan, China. *Equal contributors.

Received December 24, 2023; Accepted January 25, 2024; Epub January 25, 2024; Published January 30, 2024

Abstract: ZW10 interacting kinetochore protein (ZWINT), an essential part of the kinetochore complex, plays a crucial role in maintaining genome stability by correcting improper attachments between the kinetochore and microtubules. An initial analysis of The Cancer Genome Atlas and Gene Expression Omnibus databases revealed that ZWINT is significantly expressed across a diverse range of tumor types. We subsequently investigated the influence of ZWINT on clinical outcomes and potential signaling pathways. A multidimensional analysis of ZWINT revealed significant statistical associations between ZWINT expression and clinical outcomes, as well as the E2F1 oncogenic signature. Experimental validation confirmed the increased expression of ZWINT in both pancreatic cancer cell lines and pancreatic adenocarcinoma tissues. Furthermore, our findings indicate that ZWINT promotes the proliferation of PANC-1 cells through cell cycle regulation. This comprehensive analysis of ZWINT suggests a strong correlation between its expression and various types of tumors, especially pancreatic adenocarcinoma (PAAD), indicating its potential oncogenic role. These findings enhance our understanding of the function of ZWINT in carcinogenesis.

Keywords: ZWINT, prognosis, pancreatic adenocarcinoma, pan-cancer

Introduction

In 2000, ZW10 interacting kinetochore protein (ZWINT) was first identified by Starr et al. [1]. ZWINT is localized in the kinetochore region, which comprises several protein subunits that connect chromosomes to spindle microtubules, facilitating chromosome segregation. ZWINT is a critical component of this complex, although its specific role remains unclear [2]. Previous research has shown the dependence of both chromosome motility and spindle checkpoint control on ZWINT [3]. The E3 ubiquitin ligase Terf induces ZWINT protein degradation, thereby negatively regulating cell proliferation [4]. Furthermore, ZWINT is essential for correcting incorrect kinetochore-microtubule attachments [5]. To ensure the accurate separation of chromosomes, the spindle assembly checkpoint regulates cell division, thereby preserving the stability of the genome [6].

Chromosomal instability, characterized by errors in chromosome separation during mitosis,

is a hallmark of human cancer and correlates with poor prognosis [7]. A study identified a 70-gene chromosomal instability pattern in various cancers; among these was ZWINT [8]. Increasing evidence suggests that ZWINT is dysregulated in malignancies. High mRNA levels of ZWINT have been associated with poor prognosis in lung adenocarcinoma [9]. A tissue microarray study showed that colorectal cancer cases positive for ZWINT had significantly worse overall survival [10]. However, a multidimensional pan-cancer study of ZWINT has not yet been conducted.

Pan-cancer studies, examining genomic alterations and molecular characteristics across multiple cancer types, provide new insights into cancer diagnosis, prognosis, and treatment [11]. Our study aimed to explore the role of ZWINT in tumor progression, clinical outcomes, and signaling pathways using a pan-cancer approach. We validated ZWINT protein levels in cancer cell lines and human tumor samples using bioinformatics data and conducted an

extensive analysis of the effect of ZWINT on the cell cycle regulation in PANC-1 cells.

Materials and methods

Analysis of gene expression

RNA-seq data for various cancer types were obtained from the combined cohort of The Cancer Genome Atlas (TCGA), Therapeutically Applicable Research to Generate Effective Treatments (TARGET), and Genotype-Tissue Expression (GTEx) samples. The data were processed using the “stats” and “car” packages and visualized with the “ggplot2” package in the R platform. For external validation, we used curated gene expression datasets from the Gene Expression Omnibus (GEO) database, including GSE42568, GSE12452, GSE25097, GSE12470, and GSE15471. These datasets were processed using the ‘limma’ package to identify genes that were differentially expressed (DEGs) with a p -value < 0.05 and $|\text{Log}_2\text{Fold change}| > 1$, which were statistically significant. The Cancer Single-cell Expression Map was used to explore the cellular heterogeneity of ZWINT expression in tumors [12]. UALCAN, an interactive web tool for OMICS data analysis in cancer research [13], was used to determine the overall ZWINT protein expression levels in human tumors and normal tissues through its Clinical Proteomic Tumor Analysis Consortium (CPTAC) module.

Prognosis analysis

GEPIA2 was selected to assess the association between ZWINT expression in tumors and both overall survival (OS) and disease-free survival (DFS) [14]. The “survival” and “rms” packages in the R platform were used to create prognostic nomograms that included variables of gender, age, pathologic stage, and ZWINT expression.

Analyses of ZWINT-related proteins and genes

The STRING database (<https://string-db.org/>) was used to analyze the protein-protein interactions (PPI) of ZWINT. Proteins that interacted with ZWINT were identified in the PPI network. The GEPIA2 tool was used to examine the target genes correlated with ZWINT, focusing on the top 100 genes, through the ‘Similar Genes Detection’ module. Venn Diagrams were em-

ployed for intersection analysis of ZWINT-interacted and ZWINT-correlated genes. The common genes for intersection analysis were selected using the “Gene_Corr” module of TIMER2.0 web server to conduct Spearman correlation with ZWINT expression. Combining the datasets of ZWINT-interacted and ZWINT-correlated genes, the “clusterProfiler” package in R platform was used to conduct KEGG pathway analysis and GO enrichment analysis.

Gene set enrichment analysis of ZWINT in pancreatic cancer

To identify the cancer-causing signaling pathways in the TCGA database, we utilized Gene Set Enrichment Analysis (GSEA) by comparing the ZWINT low- and high-expression groups (using the median cutoff value). MSigDB C6 (oncogenic signature gene sets) enrichment analysis was conducted using the ‘clusterProfiler’ package in R. Significant enrichment was determined when p_{adjust} was less than 0.05, FDR was less than 0.25, and the absolute value of NES was greater than 1.

Immunohistochemical staining

Tissue samples were obtained from cancer patients who underwent surgery at the Third Xiangya Hospital of Central South University, with informed consent provided by each patient. The details of immunohistochemical staining are described in our previous publication [15]. Antibody against ZWINT (ZWINT: 1:200 dilution, ab252950, Abcam) was used for immunohistochemical staining. The intensity of ZWINT staining was quantified by an experienced pathologist. This study followed the guidelines outlined in the Declaration of Helsinki. The ethics committees of the Third Xiangya Hospital approved all experiments conducted in this study (No. 23319).

Cell culture and siRNA transfection

HPDE6-C7, PANC-1, and MIAPaCa-2 cell lines were obtained from the BeNa Culture Collection (BNCC359453, BNCC352264, BNCC337700, Beijing, China). Small interfering RNAs (siRNAs) targeting ZWINT, and an empty vector (si-NC) were synthesized by GenePharma (Shanghai, China). The information about siRNA can be found in [Table S1](#). Cell transfection was performed using Lipofectamine® 3000 (Invitro-

Multidimensional analysis of ZW10

gen/Thermo Fisher Scientific, Carlsbad, CA, USA), following the manufacturer's guidelines.

The streamlined process for siRNA transfection is as follows: Initially, PANC-1 cells were cultured in a 6-well plate. When the cell confluence approximately reached 50%, the existing medium was substituted with an antibiotic-free culture medium. Subsequently, the pre-prepared transfection complex was introduced to the cells, adhering to the dosage guidelines recommended by the manufacturer. Following this, the cells underwent a 24-hour incubation period prior to any further treatments. To assess the effectiveness of the transfection, techniques such as qPCR and Western blot were employed. Further cell culture details are available in our prior study [15].

RT-PCR

Total RNA from cells was extracted using the Steady Pure RNA Extraction Kit (Accurate Biotechnology, China), according to the manufacturer's instructions. For mRNA analysis using real-time PCR, cDNA was synthesized using the Evo M-MLV Reverse Transcription Kit (Accurate Biotechnology, China). Real-time PCR was then performed using the Premix Pro Taq HS qPCR Kit (Accurate Biotechnology, China), with gene-specific primers. Relative mRNA expression levels were normalized to GAPDH and quantified using the $2^{-\Delta\Delta CT}$ method. The PCR primers used are listed in [Table S2](#).

Cell cycle analysis

Cells were treated with 70% ethanol and stored at 4°C overnight. Ethanol was removed by centrifugation the following day and 500 μ l of propidium iodide (PI)/RNase staining solution was added. Staining was performed in the dark at 4°C for 5 minutes. Stained cells were then analyzed using a flow cytometer (BD Bioscience, NJ, USA).

CCK-8

Cell proliferation was assessed using the CCK-8 assay (Beyotime Biotechnology, China), according to the manufacturer's protocol. Cells were seeded in 96-well plates at a density of 2×10^3 cells per well one day prior to transfection or infection. Pancreatic cancer cell viability was evaluated in three independent ex-

periments with three replicates each, following treatments for 0, 24, 48, and 72 hours.

Western blot

Proteins separated by SDS-PAGE were transferred to a PVDF membrane (0.45 μ m pore size, Millipore, IPVH00010) for Western blot analysis. The membrane was blocked for 1 hour using a 5% milk solution, then incubated overnight at 4°C with primary antibodies (ZWINT at a 1:1000 dilution, ab252950 from Abcam; β -actin at a 1:1000 dilution, 20536-1-AP from Proteintech). After four washes with TBST, each lasting 10 minutes, the membrane was incubated with appropriate secondary antibodies at room temperature for 1 hour. Following secondary antibody incubation, the membrane was washed with TSBT, and staining was visualized using ECL via a Chemiluminescent Imaging System (Tanon).

Results

The abbreviations for the TCGA study are presented in [Table S3](#).

Gene expression analysis data

Analysis of the TCGA, TARGET, and GTEx databases revealed a significant increase in ZWINT mRNA levels in tumor tissues compared to normal tissues within the combined cohort (**Figure 1A**). In addition, the external GEO datasets confirmed that ZWINT mRNA was overexpressed in BRCA (GSE42568), HNSC (GSE12452), LIHC (GSE25097), OV (GSE12470), and PAAD (GSE15471) relative to adjacent normal tissues (**Figure 1B**). Single-cell data analysis showed that ZWINT was predominantly expressed in malignant cells across various cancer types, including non-small cell lung cancer (NSCLC), LUAD, LUSC, triple-negative breast cancer (TNBC), GBM, STAD, colorectal cancer (CRC), OV, PAAD, and Merkel cell carcinoma (MCC) ([Figure S1](#)). ZWINT protein levels were significantly higher in LUAD, UCEC, and HNSC compared to normal tissues, with expression correlating with tumor stages in these cancers (**Figure 2A-C**). However, no significant difference in ZWINT protein levels between tumor and normal tissues was observed in LIHC and OV (**Figure 2D, 2E**).

Multidimensional analysis of ZW10

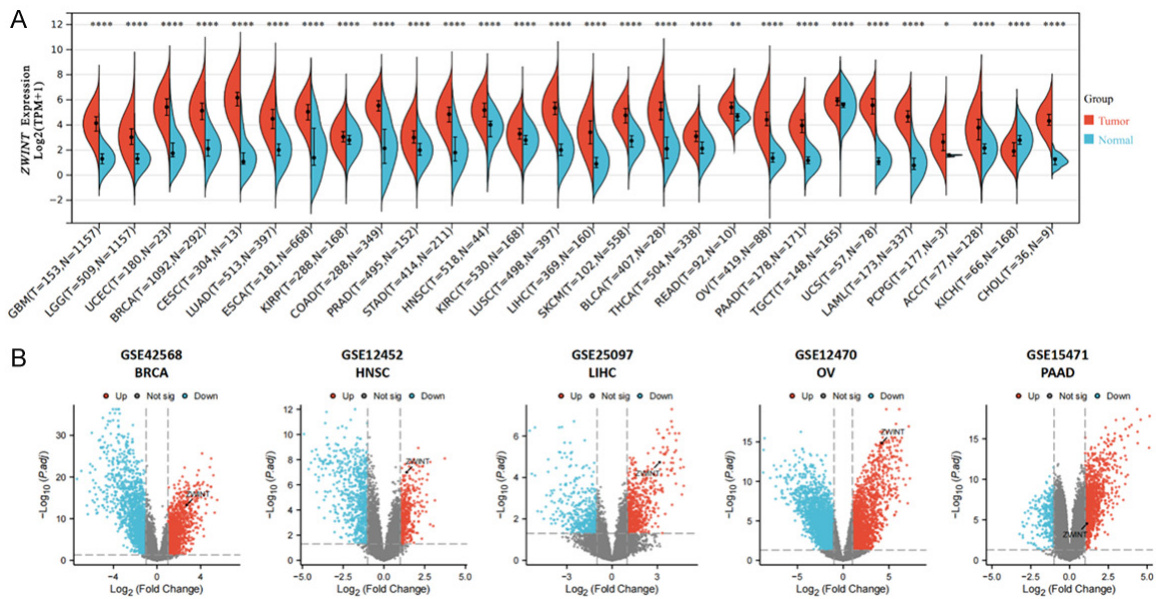


Figure 1. ZWINT mRNA levels in various tumors and normal tissues. A. A marked increase in ZWINT mRNA levels in tumor tissues compared to normal tissues in the TCGA, TARGET, and GTEx databases. B. External GEO datasets confirmed that ZWINT mRNA was overexpressed in BRCA, HNSC, LIHC, OV, and PAAD relative to adjacent normal tissues. TPM, transcripts per million; BRCA, breast invasive carcinoma; HNSC, head and neck squamous cell carcinoma; LIHC, liver hepatocellular carcinoma; OV, ovarian serous cystadenocarcinoma; PAAD, Pancreatic adenocarcinoma; * $P < 0.05$, ** $P < 0.01$, **** $P < 0.0001$.

Prognosis analysis data

To investigate the correlation between ZWINT expression and tumor prognosis, the TCGA cohort was divided into two groups based on the median cutoff value of ZWINT expression. One group had low ZWINT expression, while the other group had high ZWINT expression. High ZWINT expression was strongly associated with poor overall survival in ACC, LGG, LIHC, LUAD, MESO, PAAD, SARC, and SKCM. In contrast, low ZWINT expression correlated with poor overall survival in THYM (Figure 3A). Furthermore, high ZWINT expression was significantly related to unfavorable disease-free survival in ACC, BLCA, LIHC, MESO, PRAD, SARC, SKCM, TGCT, THCA, and UVM (Figure 3B). Nomograms were employed to predict one-year overall survival of ACC, LIHC, PAAD, and SARC, with total points calculated considering pertinent clinical factors such as gender, age, pathologic stage, and ZWINT expression. A considerable portion of the total points contributing to a prediction of unfavorable one-year overall survival was attributable to increased ZWINT expression (Figure 4).

Protein-protein interactions of ZWINT and similar genes in pan-cancer

To elucidate the potential mechanisms of ZWINT in carcinogenesis, we conducted an analysis of ZWINT-related proteins and genes. The PPI network in Figure 5A identified 50 proteins empirically validated to interact with ZWINT. In addition, the top 100 similar genes of ZWINT were identified (Table S4). In Figure 5B, DSN1, BUB1, LMNB1, NDC80, NUF2, and SPC25 were found to be shared genes between the ZWINT-interacting and ZWINT-correlated gene sets. The heatmap data in Figure 5C revealed a significant and favorable association between ZWINT expression and the expression of the six shared member genes across all types of tumors in the TCGA cohort. Gene Ontology (GO) enrichment analysis of the combined dataset revealed that genes interacting with, and correlated to, ZWINT were involved in various biological processes, including cell cycle phase transition, chromosome segregation during nuclear division, organelle division, and cell cycle checkpoint regulation. These genes had diverse molecular functions, such as microtubule and tubulin binding, ATPase activi-

Multidimensional analysis of ZW10

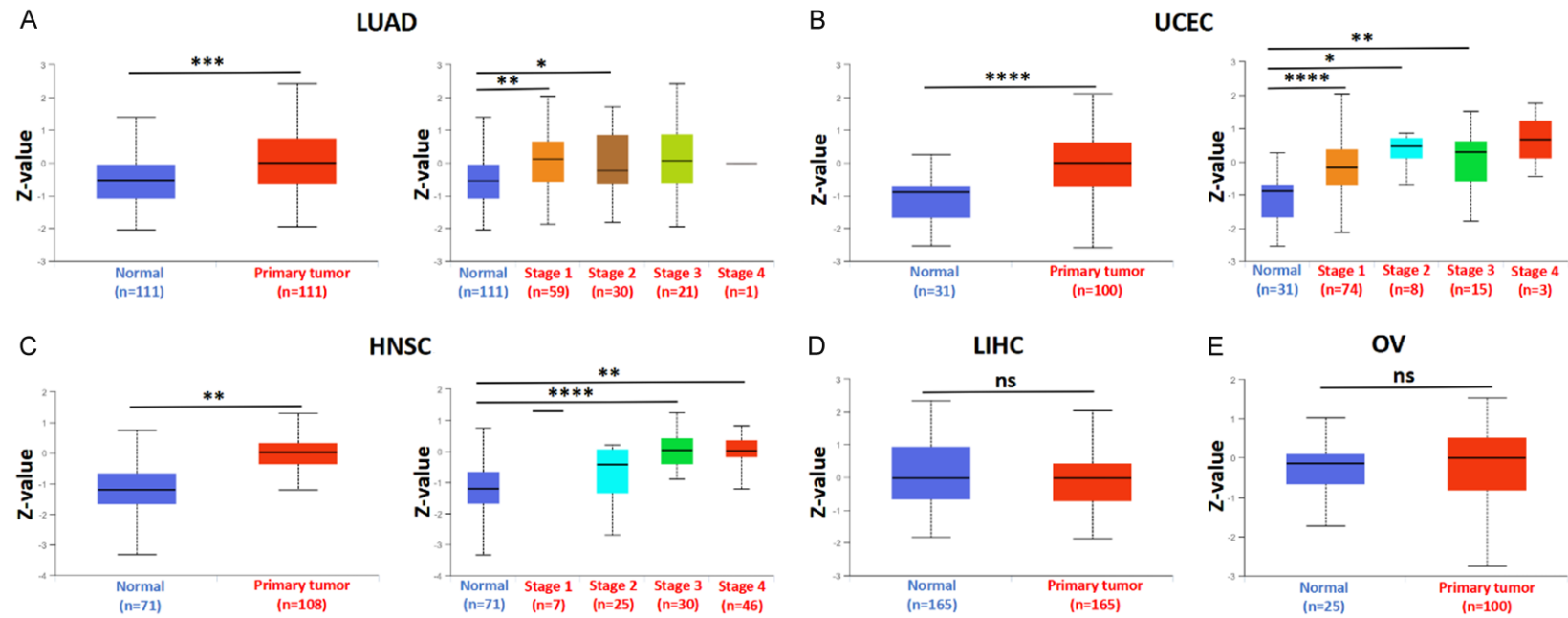
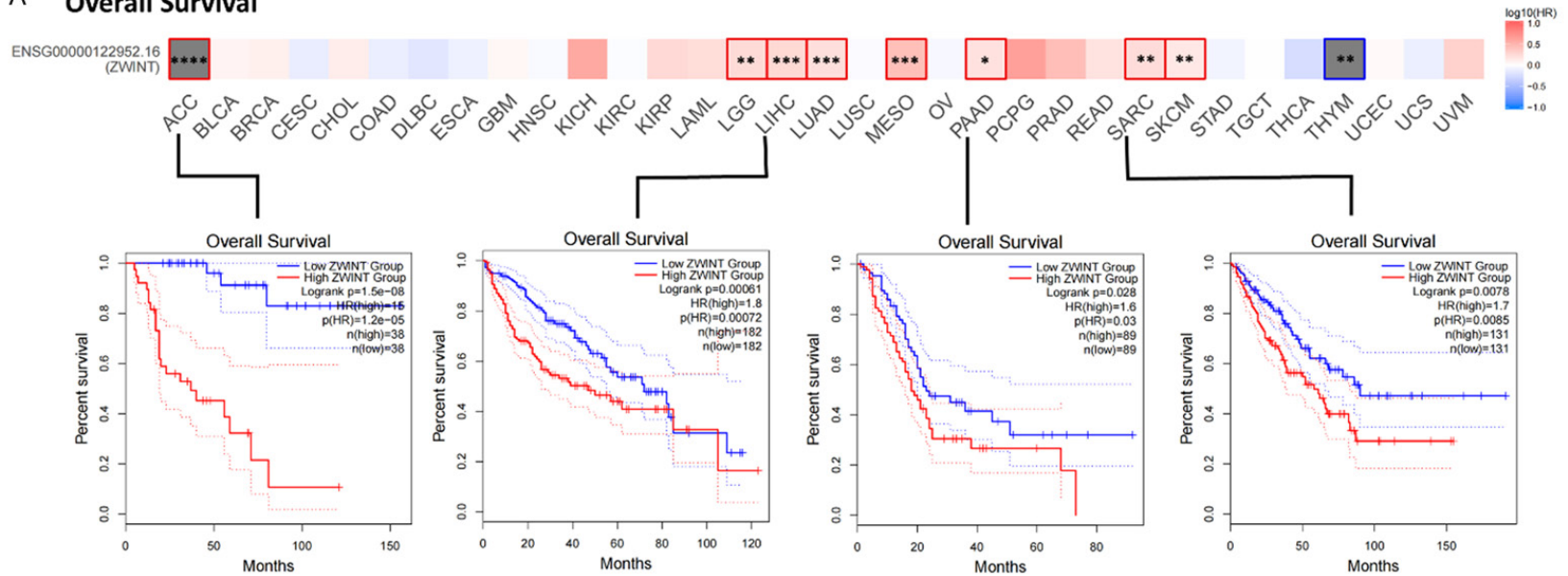


Figure 2. ZWINT protein expression in various tumors and normal tissues from the CPTAC database. ns, not significant; Z-value, represents standard deviations from the median across samples; * $P < 0.05$, ** $P < 0.01$, *** $P < 0.001$, **** $P < 0.0001$.

Multidimensional analysis of ZW10

A Overall Survival



B Disease-free survival

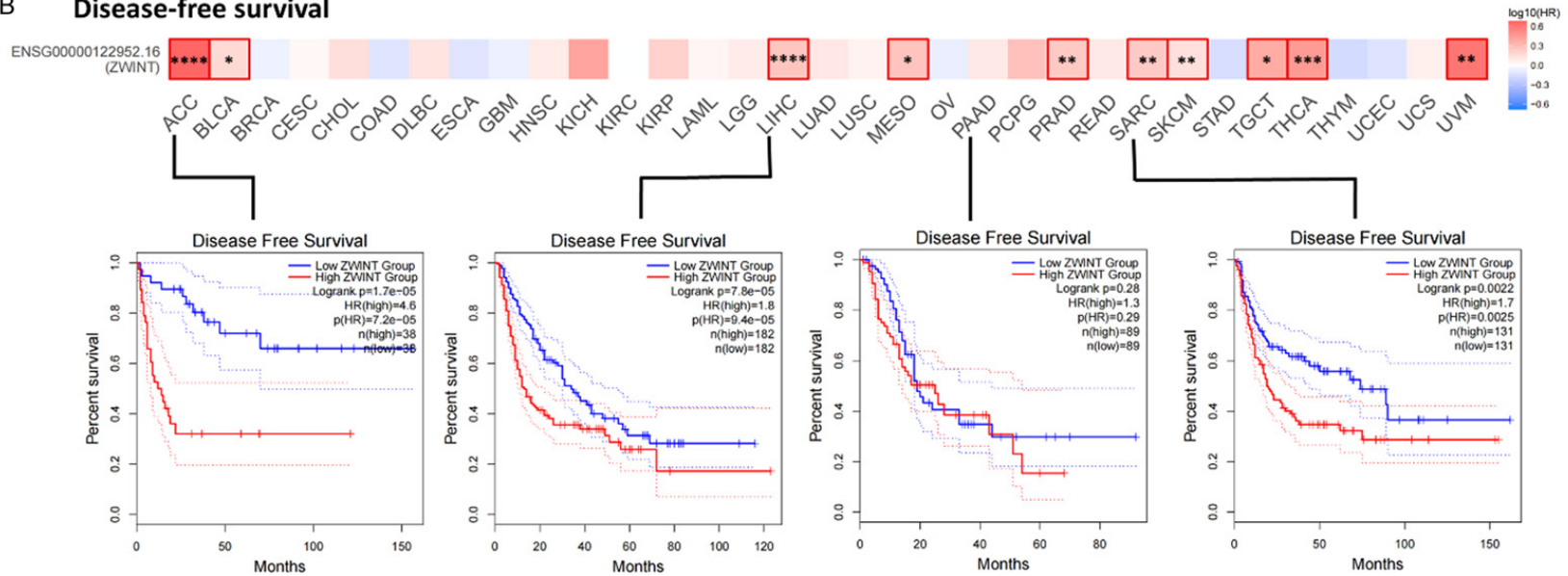


Figure 3. Relationships between ZWINT expression and prognosis of different tumors in TCGA database. HR, hazard ratio; * $P < 0.05$, ** $P < 0.01$, *** $P < 0.001$, **** $P < 0.0001$.

Multidimensional analysis of ZW10

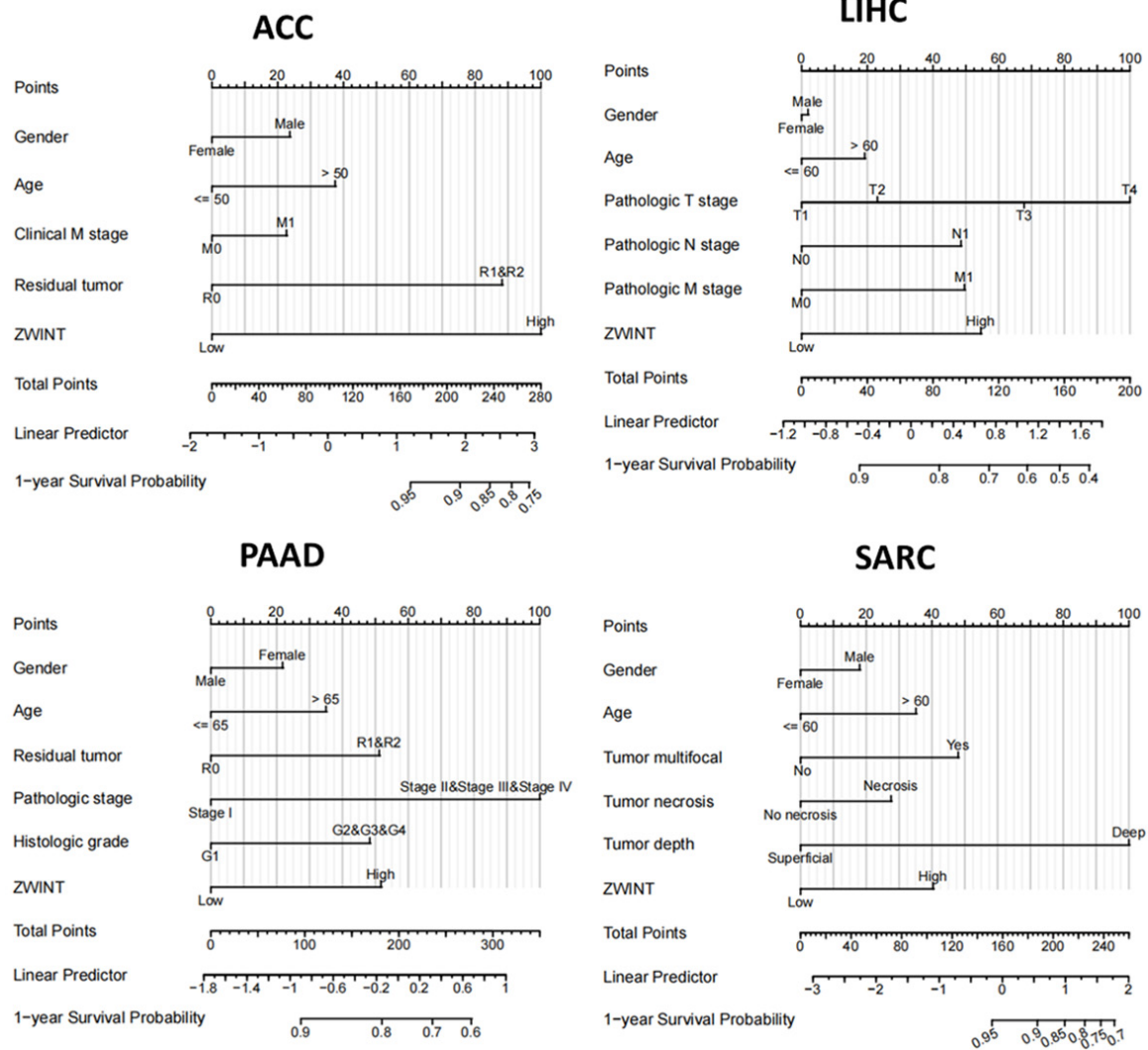


Figure 4. Nomograms for predicting one-year overall survival of ACC, LIHC, PAAD, and SARC. ACC, adrenocortical carcinoma; LIHC, liver hepatocellular carcinoma; PAAD, pancreatic adenocarcinoma; SARC, sarcoma.

ty, protein serine/threonine kinase activity, and catalytic activity. These genes were closely associated with cellular structures such as chromosomes, spindles, kinetochores, and microtubules. Moreover, KEGG pathway analysis revealed that ZWINT was involved in several pathways, including the cell cycle, DNA replication, autophagy, p53 signaling pathway, and mismatch repair (**Figure 5D**).

Data for gene set enrichment analysis

Evaluation of the C6 oncogenic signature gene sets in the Molecular Signatures Database (MSigDB) indicated that increased ZWINT levels in BLCA, CESC, ESCA, GBM, KIRP, HNSC,

LIHC, LGG, LUSC, OV, PAAD, and SARC were associated with genes that were activated due to the overexpression of the oncogene E2F1 (**Figure 6**).

Experimental validation

To validate the ZWINT expression observed in bioinformatics data, we conducted immunohistochemical staining, Western blot, and q-RT-PCR analyses to assess ZWINT expression levels in tumors. Our findings revealed a marked overexpression of ZWINT in PAAD compared to adjacent normal tissues. In contrast, no significant difference in ZWINT expression was observed between tumor tissues and adjacent

Multidimensional analysis of ZW10

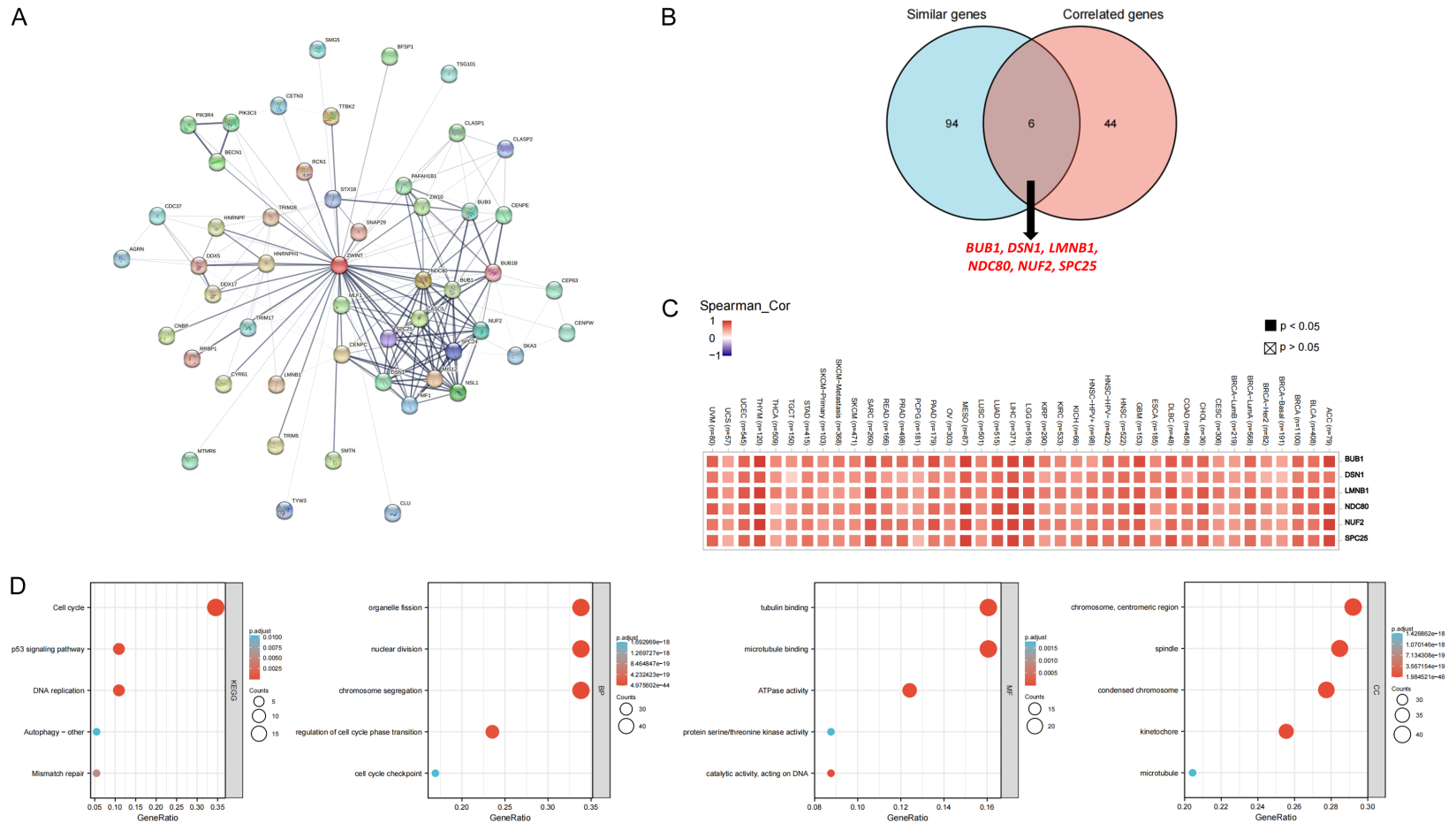


Figure 5. Analyses of ZW10-related proteins and genes. A. Protein-protein interactions identified 50 ZW10-interacting proteins in STRING. B. An intersection analysis of the ZW10-interacting and -correlated genes using a Venn Diagram. C. Correlations between ZW10 and six common genes expression in pan-cancer. D. GO enrichment and KEGG pathway analyses based on combined datasets of ZW10-interacted and ZW10-correlated genes.

Multidimensional analysis of ZW10

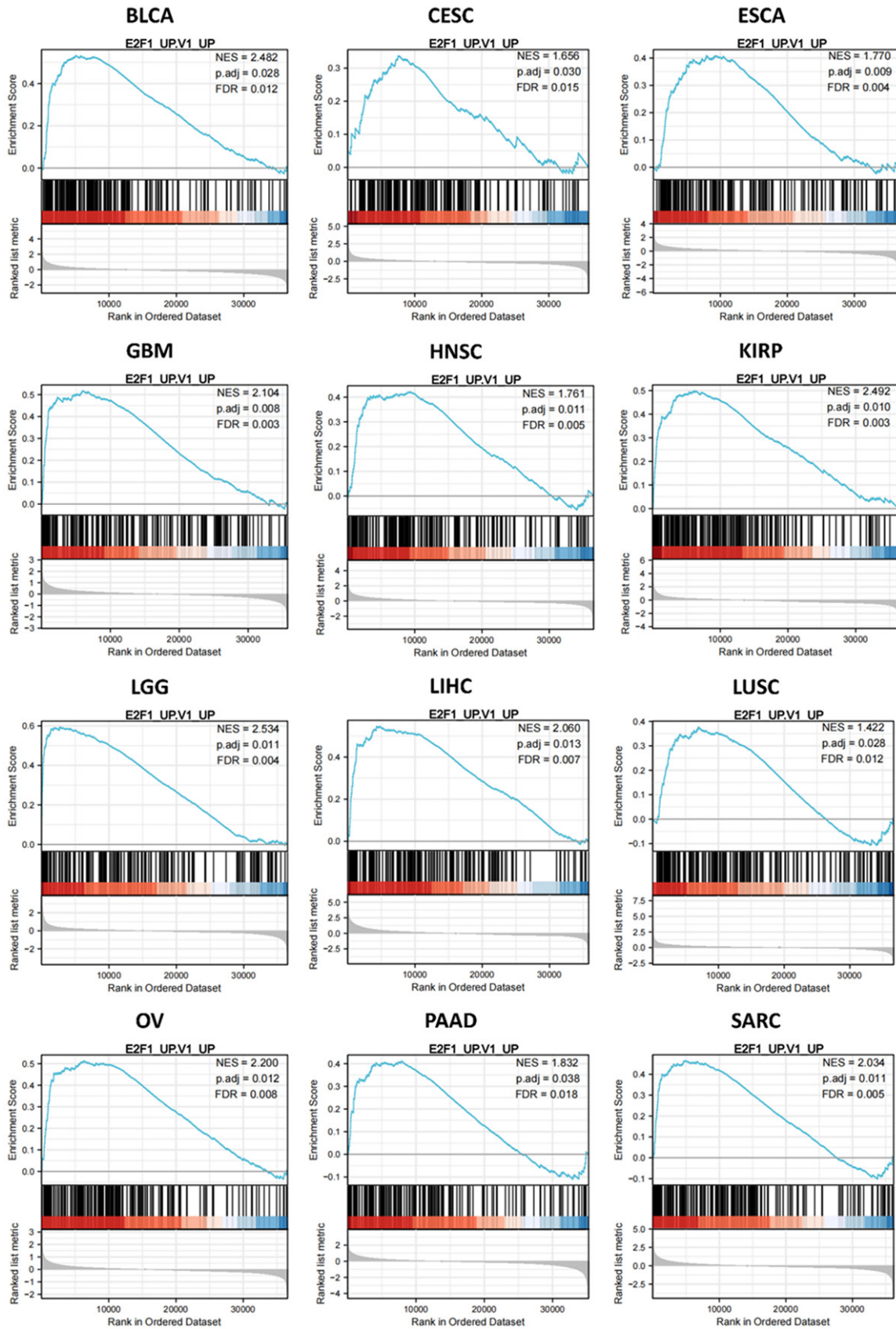
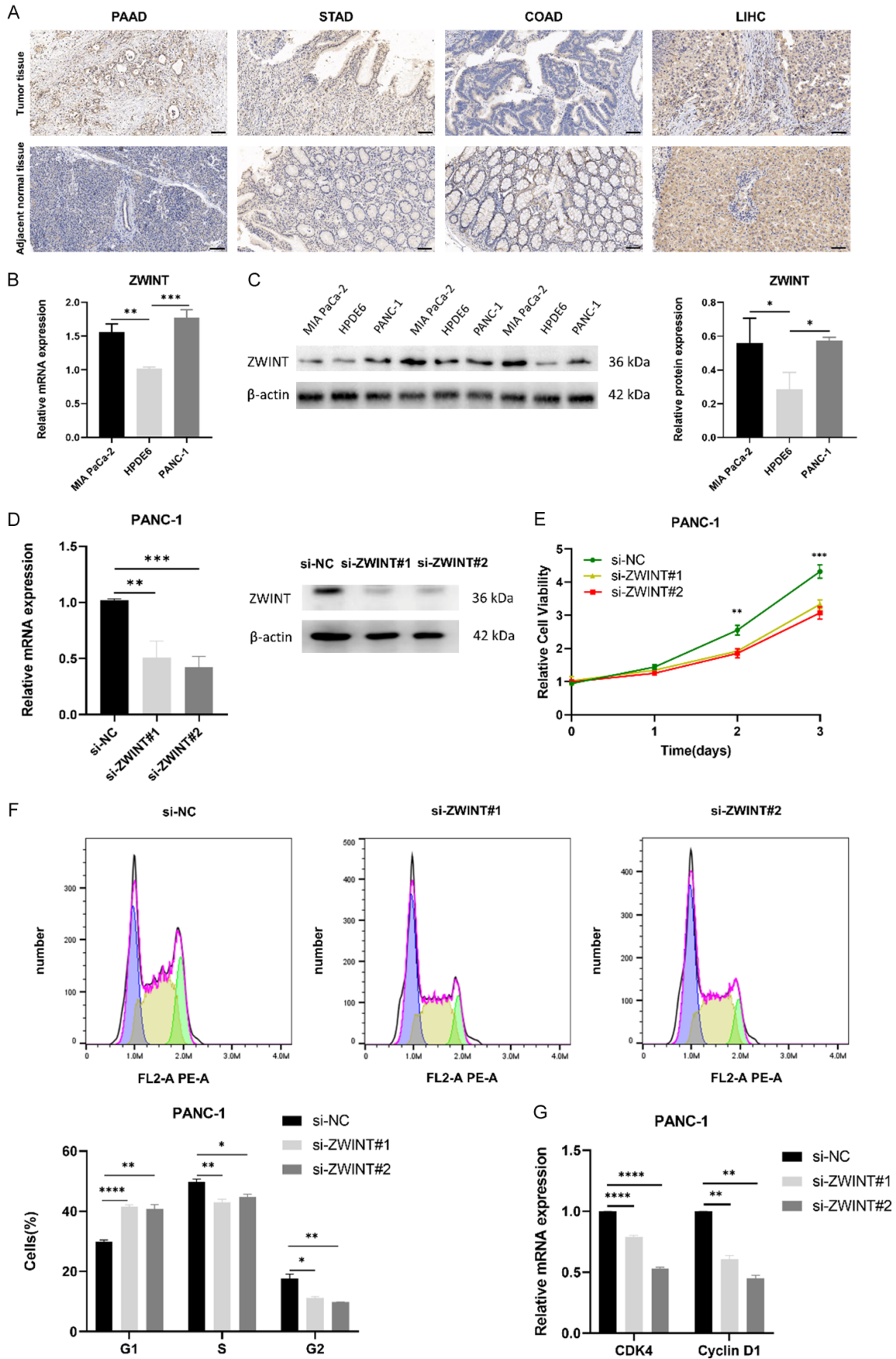


Figure 6. Oncogenic signature gene sets enrichment analysis of ZWINT. NES, normalized enrichment score; FDR, false discovery rate.

Multidimensional analysis of ZW10



Multidimensional analysis of ZW10

Figure 7. ZWINT expression in human tissues and cancer cell lines. A. ZWINT expression in PAAD, STAD, COAD, and LIHC compared with adjacent normal tissue (bar size 100 μm). B. ZWINT mRNA expression in HPDE6-C7, PANC-1, and MIA PaCa-2 cell lines. C. ZWINT protein expression in HPDE6-C7, PANC-1, and MIA PaCa-2 cell lines. D. q-RT-PCR and WB confirmed the knockdown of ZWINT. E. Growth curves of PANC-1 cells determined by CCK-8 assay. F. Cell cycle analysis showing the effect of ZWINT on the regulation of the PANC-1 cell cycle. G. q-RT-PCR analysis of cell cycle-associated genes expression. PAAD, pancreatic adenocarcinoma; STAD, stomach adenocarcinoma; COAD, Colon adenocarcinoma; LIHC, liver hepatocellular carcinoma; * $P < 0.05$, ** $P < 0.01$, *** $P < 0.001$, **** $P < 0.0001$.

normal tissues in STAD, COAD, and LIHC (**Figure 7A**). In addition, the pancreatic cancer cell lines PANC-1 and MIA PaCa-2 exhibited a significant increase in both ZWINT protein and mRNA levels, as shown by Western blot analysis and q-RT-PCR, respectively, when compared to the normal pancreatic cell line HPDE6 (**Figure 7B, 7C**). To elucidate the function of ZWINT in PANC-1 cells, we conducted experiments to inhibit ZWINT activity. q-RT-PCR and WB results confirmed successful downregulation of ZWINT in PANC-1 cell lines (**Figure 7D**), and CCK-8 assays indicated a reduction in PANC-1 cell proliferation following ZWINT knockdown (**Figure 7E**). Subsequently, we examined the involvement of ZWINT in cell cycle regulation in PANC-1 cells through flow cytometry. In ZWINT-knockdown groups, there was a notable increase in the G1 phase and a decrease in the S and G2 phases compared to the control group (**Figure 7F**). ZWINT was found to enhance the expression of genes associated with the cell cycle, as demonstrated by q-RT-PCR (**Figure 7G**).

Discussion

This study demonstrated that: (1) the mRNA level of ZWINT was markedly increased in various type of tumors based on TCGA database and GEO datasets; (2) high expression of ZWINT protein was observed in LUAD, UCEC, and HNSC according to CPTAC data; (3) elevated levels of ZWINT expression were associated with poor overall survival and disease-free survival in different types of tumors, including ACC, LIHC, MESO, SARC, and SKCM; (4) expression of BUB1, DSN1, LMNB1, NDC80, NUF2, and SPC25 was positively associated with expression of ZWINT across all TCGA cancers; (5) high ZWINT expression was linked to oncogenes of the E2F1 signature in BLCA, CESC, ESCA, HNSC, GBM, KIRP, LIHC, LGG, LUSC, OV, PAAD, and SARC; (6) experimental validation demonstrated significant overexpression of ZWINT in PAAD compared to adjacent normal tissues, highlighting its crucial role in regulating the cell cycle of tumor cells.

ZWINT is essential for the accurate arrangement and segregation of chromosomes in the process of cellular division [16]. Research indicates that disrupted expression or function of ZWINT can lead to errors in chromosomal separation and aneuploidy, both associated with cancer progression [5, 17]. A 70-gene signature of chromosomal instability, including ZWINT, was identified in various cancers [8]. The expression of ZWINT is upregulated in LIHC, and high-level expression could predict a poor prognosis [18]. In a study of 2,847 individuals with LUAD, increased ZWINT levels correlated with advanced TNM stages and a poor prognosis [19]. Additionally, ZWINT expression increased in chronic lymphocytic leukemia cells from lymph nodes, where higher expression was associated with a poor prognosis [20]. Previous research also discovered that ZWINT is highly expressed in melanoma cells and tissues, they found that knocking down ZWINT in A375 melanoma cells inhibited their proliferation and migration, suggesting ZWINT may act as an oncogene in melanoma through regulating c-Myc expression [21]. Meanwhile, additional evidence indicates that ZWINT, upregulated in GBM, significantly correlates with the kinetochore protein NDC80 and the kinase PLK1, thereby playing a crucial role in mitosis and cell cycle regulation. Knockdown of ZWINT in GBM cells led to reduced cell proliferation and invasion and increased apoptosis, both in vitro and in vivo. This study suggests that ZWINT could be a potential biomarker and therapeutic target for GBM treatment [22]. This pan-cancer study revealed that both transcriptional and translational levels of ZWINT were significantly increased in tumor tissues compared to normal tissue based on TCGA, GEO and CPTAC databases, which aligns with previous research findings. Our experimental validation showed that ZWINT was markedly overexpressed in PAAD relative to adjacent normal tissues and conducted an extensive analysis of the effect of ZWINT on the cell cycle regulation in PANC-1 cells.

In the TCGA cohort, the present investigation discovered six proteins (BUB1, DSN1, LMNB1, NDC80, NUF2, and SPC25) that had experimental interactions with ZWINT. Additionally, the expression of ZWINT in all types of tumors demonstrated a positive correlation with these six genes. Notably, the interaction between ZWINT and the six proteins (BUB1, DSN1, LMNB1, NDC80, NUF2, and SPC25) was detected through tandem affinity purification assay, identifying them as chromosome segregation proteins [23]. Overexpression of BUB1, which can induce aneuploidy and cancer formation, suggests its oncogenic properties [24]. The expression of BUB1 and ZWINT was markedly upregulated in LUAD and PAAD, as evidenced by DNA microarray analysis [25]. DSN1, a component of the minichromosome instability-12 centromere complex, is essential for proper kinetochore formation and cell cycle progression [26]. DSN1 acts as a critical downstream target of serine/arginine-rich splicing factor 9, facilitating COAD progression [27]. The presence of LMNB1 in the nuclear lamina has been linked to the development, aggressiveness, and metastasis of cancer [28]. NDC80, an essential element in the clustering of centrosomes, plays a significant role in promoting chromosomal instability and cancer progression [29]. NUF2, a component of the NDC80 kinetochore complex, is involved in the initiation and advancement of CHOL and KIRC [30, 31]. SPC25, another component of the NDC80 kinetochore complex, is essential for spindle checkpoint function and chromosome separation. Studies have shown that SPC25 promotes the proliferation and stemness of hepatocellular carcinoma cells [32]. However, there is still limited research on the roles of the interaction between ZWINT and six proteins (BUB1, DSN1, LMNB1, NDC80, NUF2, and SPC25) in tumorigenesis. In addition, GSEA analysis in this study suggests that ZWINT may share similar functions with the oncogene E2F1.

In conclusion, this pan-cancer analysis of ZWINT reveals a strong correlation with various tumor types, suggesting its potentially function as an oncogene. These findings enhance our understanding of the function of ZWINT in carcinogenesis.

Disclosure of conflict of interest

None.

Address correspondence to: Dr. Chao Deng, Department of Orthopedics, Xiangya Hospital, Central South University, Changsha 410008, Hunan, China. E-mail: orthodengchao@foxmail.com

References

- [1] Starr DA, Saffery R, Li Z, Simpson AE, Choo KH, Yen TJ and Goldberg ML. HZwint-1, a novel human kinetochore component that interacts with HZW10. *J Cell Sci* 2000; 113: 1939-50.
- [2] Petrovic A, Keller J, Liu Y, Overlack K, John J, Dimitrova YN, Jenni S, van Gerwen S, Stege P, Wohlgemuth S, Rombaut P, Herzog F, Harrison SC, Vetter IR and Musacchio A. Structure of the MIS12 complex and molecular basis of its interaction with CENP-C at human kinetochores. *Cell* 2016; 167: 1028-1040, e15.
- [3] Lin YT, Chen Y, Wu G and Lee WH. Hec1 sequentially recruits Zwint-1 and ZW10 to kinetochores for faithful chromosome segregation and spindle checkpoint control. *Oncogene* 2006; 25: 6901-14.
- [4] Endo H, Ikeda K, Urano T, Horie-Inoue K and Inoue S. Terf/TRIM17 stimulates degradation of kinetochore protein ZWINT and regulates cell proliferation. *J Biochem* 2012; 151: 139-44.
- [5] Woo Seo D, Yeop You S, Chung WJ, Cho DH, Kim JS and Su Oh J. Zwint-1 is required for spindle assembly checkpoint function and kinetochore-microtubule attachment during oocyte meiosis. *Sci Rep* 2015; 5: 15431.
- [6] Lara-Gonzalez P, Westhorpe FG and Taylor SS. The spindle assembly checkpoint. *Curr Biol* 2012; 22: R966-80.
- [7] Bakhoun SF and Cantley LC. The multifaceted role of chromosomal instability in cancer and its microenvironment. *Cell* 2018; 174: 1347-60.
- [8] Carter SL, Eklund AC, Kohane IS, Harris LN and Szallasi Z. A signature of chromosomal instability inferred from gene expression profiles predicts clinical outcome in multiple human cancers. *Nat Genet* 2006; 38: 1043-8.
- [9] Endoh H, Tomida S, Yatabe Y, Konishi H, Osada H, Tajima K, Kuwano H, Takahashi T and Mitsudomi T. Prognostic model of pulmonary adenocarcinoma by expression profiling of eight genes as determined by quantitative real-time reverse transcriptase polymerase chain reaction. *J Clin Oncol* 2004; 22: 811-9.
- [10] Akabane S, Oue N, Sekino Y, Asai R, Thang PQ, Taniyama D, Sentani K, Yukawa M, Toda T, Kimura KI, Egi H, Shimizu W, Ohdan H and Yasui W. KIFC1 regulates ZWINT to promote tumor progression and spheroid formation in colorectal cancer. *Pathol Int* 2021; 71: 441-52.

Multidimensional analysis of ZW10

- [11] Chen F, Wendl MC, Wyczalkowski MA, Bailey MH, Li Y and Ding L. Moving pan-cancer studies from basic research toward the clinic. *Nat Cancer* 2021; 2: 879-90.
- [12] Zeng J, Zhang Y, Shang Y, Mai J, Shi S, Lu M, Bu C, Zhang Z, Zhang Z, Li Y, Du Z and Xiao J. CancerSCEM: a database of single-cell expression map across various human cancers. *Nucleic Acids Res* 2022; 50: D1147-D1155.
- [13] Zhang Y, Chen F, Chandrashekar DS, Varambally S and Creighton CJ. Proteogenomic characterization of 2002 human cancers reveals pan-cancer molecular subtypes and associated pathways. *Nat Commun* 2022; 13: 2669.
- [14] Tang Z, Kang B, Li C, Chen T and Zhang Z. GEPIA2: an enhanced web server for large-scale expression profiling and interactive analysis. *Nucleic Acids Res* 2019; 47: W556-W560.
- [15] Zhang B, Hu Q, Li Y, Xu C, Xie X, Liu P, Xu M, Gong S and Wu H. Diaphanous-related formin subfamily: novel prognostic biomarkers and tumor microenvironment regulators for pancreatic adenocarcinoma. *Front Mol Biosci* 2022; 9: 910950.
- [16] Kops GJ, Kim Y, Weaver BA, Mao Y, McLeod I, Yates JR 3rd, Tagaya M and Cleveland DW. ZW10 links mitotic checkpoint signaling to the structural kinetochore. *J Cell Biol* 2005; 169: 49-60.
- [17] Famulski JK, Vos L, Sun X and Chan G. Stable hZW10 kinetochore residency, mediated by hZwint-1 interaction, is essential for the mitotic checkpoint. *J Cell Biol* 2008; 180: 507-20.
- [18] Ying H, Xu Z, Chen M, Zhou S, Liang X and Cai X. Overexpression of Zwint predicts poor prognosis and promotes the proliferation of hepatocellular carcinoma by regulating cell-cycle-related proteins. *Onco Targets Ther* 2018; 11: 689-702.
- [19] Zhu R, Wang H and Lin L. Prognostic and clinicopathological value of ZWINT expression levels in patients with lung adenocarcinoma: a systematic review and meta-analysis. *Clinics (Sao Paulo)* 2021; 76: e3222.
- [20] Gilling CE, Mittal AK, Chaturvedi NK, Iqbal J, Aoun P, Bierman PJ, Bociek RG, Weisenburger DD and Joshi SS. Lymph node-induced immune tolerance in chronic lymphocytic leukaemia: a role for caveolin-1. *Br J Haematol* 2012; 158: 216-31.
- [21] Ma Z, Cai Y and Tian C. ZWINT promotes the proliferation, migration, and invasion of cervical cancer cells by regulating the p53/p21 signaling pathway. *Chin J Physiol* 2023; 66: 372-78.
- [22] Yang L, Han N, Zhang X, Zhou Y, Chen R and Zhang M. ZWINT: a potential therapeutic biomarker in patients with glioblastoma correlates with cell proliferation and invasion. *Oncol Rep* 2020; 43: 1831-1844.
- [23] Hutchins JR, Toyoda Y, Hegemann B, Poser I, Hériché JK, Sykora MM, Augsburg M, Hudecz O, Buschhorn BA, Bulkescher J, Conrad C, Comartin D, Schleiffer A, Sarov M, Pozniansky A, Slabicki MM, Schloissnig S, Steinmacher I, Leuschner M, Ssykor A, Lawo S, Pelletier L, Stark H, Nasmyth K, Ellenberg J, Durbin R, Buchholz F, Mechtler K, Hyman AA and Peters JM. Systematic analysis of human protein complexes identifies chromosome segregation proteins. *Science* 2010; 328: 593-9.
- [24] Ricke RM, Jeganathan KB and van Deursen JM. Bub1 overexpression induces aneuploidy and tumor formation through Aurora B kinase hyperactivation. *J Cell Biol* 2011; 193: 1049-64.
- [25] Hamada K, Ueda M, Satoh M, Inagaki N, Shimada H and Yamada-Okabe H. Increased expression of the genes for mitotic spindle assembly and chromosome segregation in both lung and pancreatic carcinomas. *Cancer Genomics Proteomics* 2004; 1: 231-40.
- [26] Kline SL, Cheeseman IM, Hori T, Fukagawa T and Desai A. The human Mis12 complex is required for kinetochore assembly and proper chromosome segregation. *J Cell Biol* 2006; 173: 9-17.
- [27] Wang X, Lu X, Wang P, Chen Q, Xiong L, Tang M, Hong C, Lin X, Shi K, Liang L and Lin J. SRSF9 promotes colorectal cancer progression via stabilizing DSN1 mRNA in an m6A-related manner. *J Transl Med* 2022; 20: 198.
- [28] Evangelisti C, Rusciano I, Mongiorgi S, Ramazzotti G, Lattanzi G, Manzoli L, Cocco L and Ratti S. The wide and growing range of lamin B-related diseases: from laminopathies to cancer. *Cell Mol Life Sci* 2022; 79: 126.
- [29] Leber B, Maier B, Fuchs F, Chi J, Riffel P, Anderhub S, Wagner L, Ho AD, Salisbury JL, Boutros M and Krämer A. Proteins required for centrosome clustering in cancer cells. *Sci Transl Med* 2010; 2: 33ra38.
- [30] Shan J, Jiang W, Chang J, Zhou T, Chen Y, Zhang Y, Wang J, Wang Y, Wang Y, Xu X, Liu S, Shi X, Fan S, Chen R, Li C and Li X. NUF2 drives cholangiocarcinoma progression and migration via inhibiting autophagic degradation of TFR1. *Int J Biol Sci* 2023; 19: 1336-51.
- [31] Lin J, Chen X, Yu H, Min S, Chen Y, Li Z and Xie X. NUF2 drives clear cell renal cell carcinoma by activating HMGA2 transcription through KDM2A-mediated H3K36me2 demethylation. *Int J Biol Sci* 2022; 18: 3621-35.
- [32] Yang J, Huang Y, Song M, Pan Q, Zhao J, He J, Ouyang D, Yang C, Han Y, Tang Y, Wang Q, He J, Li Y, Chen H, Weng D, Xiang T and Xia J. SPC25 promotes proliferation and stemness of hepatocellular carcinoma cells via the DNA-PK/AKT/Notch1 signaling pathway. *Int J Biol Sci* 2022; 18: 5241-59.

Multidimensional analysis of ZW10

Table S1. The siRNA information

Gene Name	Sequence
ZWINT-NC	Sense: 5'-UUCUCCGAACGUGUCACGUTT-3' Antisense: 5'-ACGUGACACGUUCGGAGAATT-3'
ZWINT-homo-94(#1)	Sense: 5'-GGCAGGCAUCUUGGAACCU-3' Antisense: 5'-AGGUUCCAAGAUGCCUGCCTT-3'
ZWINT-homo-301(#2)	Sense: 5'-GGCAAUUGCAGCUAAGGAATT-3' Antisense: 5'-UUCUUAGCUGCAAUUGCCTT-3'

Table S2. The primers used in the q-RT-PCR reaction

Gene Name	Sequence
GAPDH	F: 5'-ACAACCTTTGGTATCGTGAAGG-3' R: 5'-GCCATCACGCCACAGTTTC-3'
ZWINT	F: 5'-AGGACTGCTAAGGGTCTCG-3' R: 5'-GCCTCTACGTCTCCCTGTA-3'
CDK4	F: 5'-ATGGCTACCTCTCGATATGAGC-3' R: 5'-CATTGGGGACTCTCACACTCT-3'
Cyclin D1	F: 5'-GCTGCGAAGTGAAACCATC-3' R: 5'-CCTCCTTCTGCACACATTGAA-3'

Table S3. TCGA study abbreviations

Study Abbreviation	Study name
ACC	Adrenocortical carcinoma
BLCA	Bladder Urothelial Carcinoma
LGG	Brain Lower Grade Glioma
BRCA	Breast invasive carcinoma
CESC	Cervical squamous cell carcinoma and endocervical adenocarcinoma
CHOL	Cholangiocarcinoma
COAD	Colon adenocarcinoma
ESCA	Esophageal carcinoma
GBM	Glioblastoma multiforme
HNSC	Head and Neck squamous cell carcinoma
KIRC	Kidney renal clear cell carcinoma
KIRP	Kidney renal papillary cell carcinoma
LIHC	Liver hepatocellular carcinoma
LUAD	Lung adenocarcinoma
LUSC	Lung squamous cell carcinoma
MESO	Mesothelioma
OV	Ovarian serous cystadenocarcinoma
PAAD	Pancreatic adenocarcinoma
PRAD	Prostate adenocarcinoma
SARC	Sarcoma
SKCM	Skin Cutaneous Melanoma
STAD	Stomach adenocarcinoma
TGCT	Testicular Germ Cell Tumors
THYM	Thymoma
THCA	Thyroid carcinoma
UCEC	Uterine Corpus Endometrial Carcinoma
UVM	Uveal Melanoma

Multidimensional analysis of ZW10

Table S4. ZWINT correlated and similar genes based on String, and GEPIA2

Similar genes	Correlated genes
CDK1	AGRN
KIF11	BECN1
KIFC1	BFSP1
NCAPH	BUB1
DNAJC9	BUB1B
NUSAP1	BUB3
KIF2C	CASC5
TIMELESS	CDC37
KIF4A	CENPC
FEN1	CENPE
LMNB1	CENPW
NEK2	CEP63
UBE2T	CETN3
CDCA5	CLASP1
CDC25C	CLASP2
PLK4	CLU
MCM6	CNBP
CCNB1	CYR61
CCNB2	DDX17
RACGAP1	DDX5
PRC1	DSN1
PCNA	HNRNPF
NCAPG	HNRNPH1
EXO1	LMNB1
CENPF	MIS12
KIF23	MLF1
GINS1	MTMR6
MKI67	NDC80
CCNF	NSL1
TPX2	NUF2
KIF15	PAFAH1B1
SKA1	PIK3C3
DLGAP5	PIK3R4
CCNA2	PMF1
CENPI	RCN1
OIP5	RRBP1
MCM2	SKA3
SGOL1	SMG5
DTL	SMTN
MELK	SNAP29
GTSE1	SPC24
DSN1	SPC25
TTK	STX18
NUF2	TRIM17
FANCI	TRIM28
ASF1B	TRIM5
MCM3	TSG101
ASPM	TTBK2

Multidimensional analysis of ZW10

CHAF1B	TYW3
CEP55	ZW10
KIF20A	
PLK1	
CENPU	
BUB1	
RRM2	
MAD2L1	
NCAPG2	
CHEK1	
MCM10	
MIS18A	
EZH2	
KIAA0101	
TMPO	
ZWILCH	
BIRC5	
POC1A	
CDCA8	
LRR1	
SPC25	
RRM1	
RAD54L	
TROAP	
KPNA2	
CENPA	
NDC80	
HJURP	
SRSF7	
ESPL1	
WDR76	
RFC5	
ORC6	
RAD51	
DONSON	
KIF14	
C16orf59	
FAM111B	
AURKB	
GINS2	
HMMR	
KIAA1524	
CHAF1A	
AUNIP	
SRSF3	
KIF18A	
CDCA3	
SASS6	
TCF19	
KIF18B	
CKAP2L	
CDC45	

Multidimensional analysis of ZW10

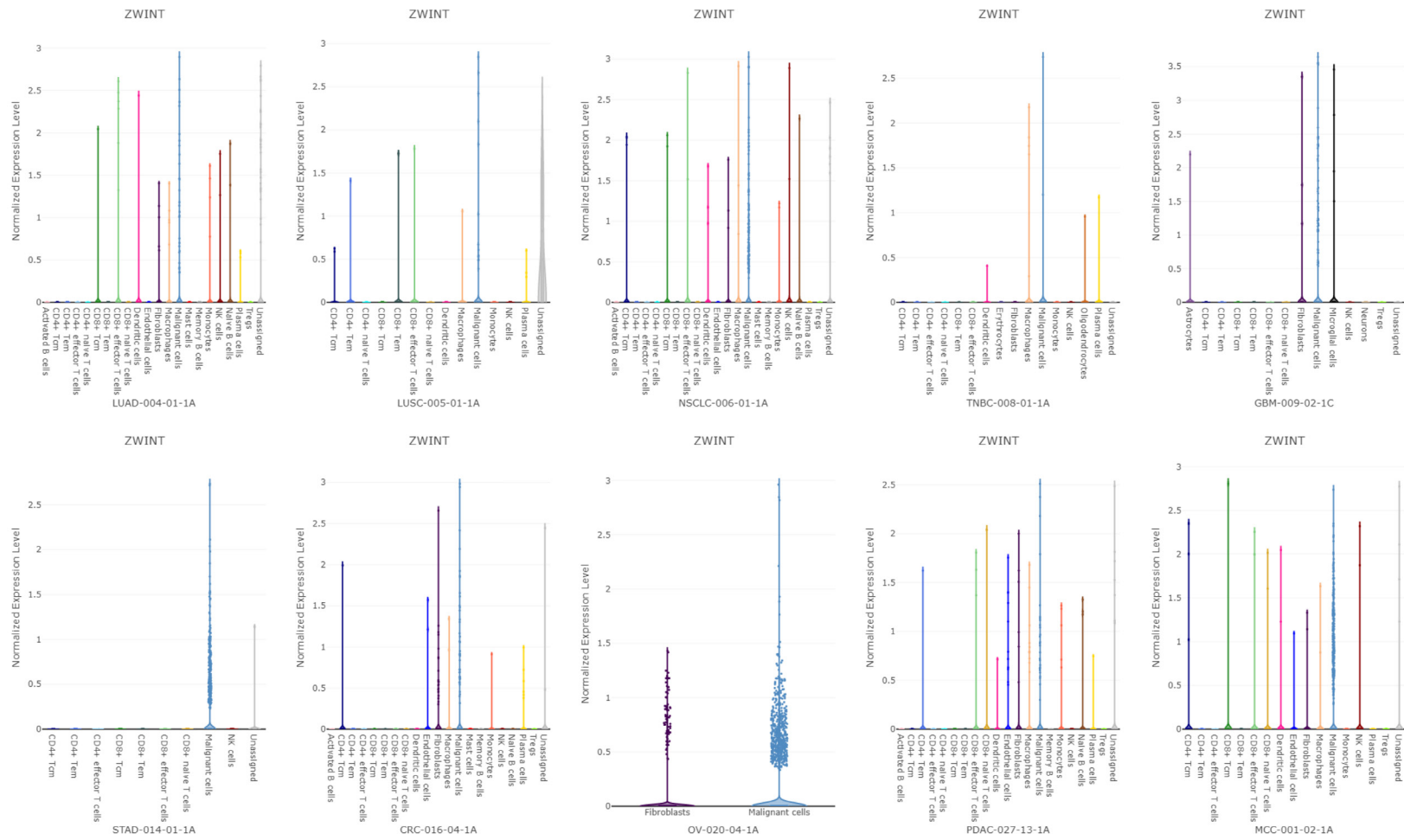


Figure S1. Single-cell data analysis of ZW10 expression in tumors.